lajss.org© Latin American Journal of Solids and Structures
www.lajss.org

Dynamic response of piled structures including pile–soil–pile interaction

Amanda Oliveira[a]*, Ana Carolina Azevedo Vasconcelos[a], Josué Labaki[a]

[a]Faculdade de Engenharia Mecânica, Universidade Estadual de Campinas, R. Mendeleyev 200, Cidade Universitária Zeferino Vaz, 13083-860, Campinas, SP, Brasil. E-mail: a261912@dac.unicamp.br, a.c.azevedovasconcelos@tudelft.nl, labaki@unicamp.br.

*Corresponding author

https://doi.org/10.1590/1679-78257514

Abstract

This article presents a numerical model and analyses of the dynamic response of structures supported by groups of piles. The model uses a finite element discretization to represent arbitrarily-shaped structures, and a coupled finite-boundary element scheme to represent the embedded pile group. This scheme properly takes into account the energy transferred from the structure to the piles and between piles through the soil, so that the effect of dynamic pile–soil–pile interaction in the response of the structure can be studied. The model is used to analyze the dynamic response of a wind turbine tower and foundation blocks of various designs. The results show that some common design approximations may result in considerable misrepresentation of the response of these structures. The model is also used to analyze cases in which the only source of excitation to a structure comes through the soil from neighboring structures. The results showed that the farther the structure is from the source of vibration, the lower its amplitude of vibration and that the taller the structure, the lower its resonant frequencies. These analyses are only possible with models like the one presented in this article, which are able to describe the energy exchanged through the soil by the piles in a group.

Keywords

Pile groups, Soil-structure interaction, Geotechnics, Coupled methods.

Graphical Abstract

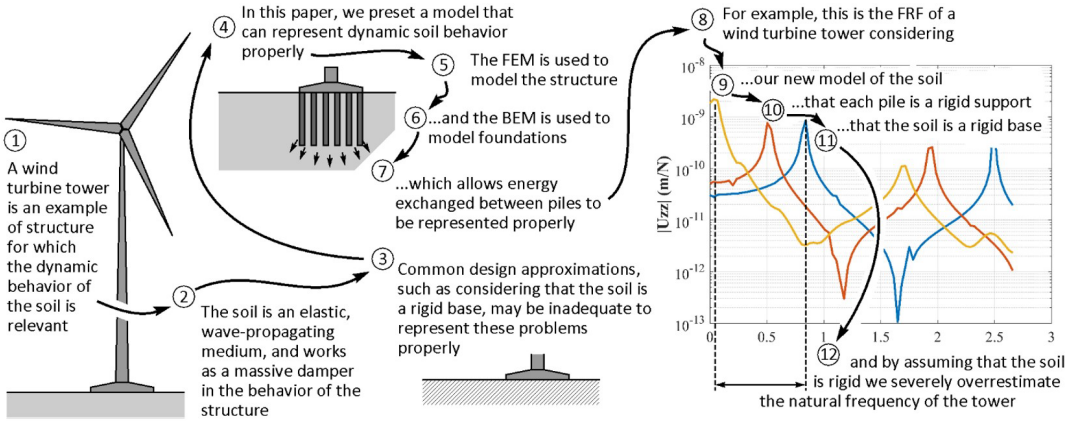

Received: February 15, 2023. In revised form: May 06, 2023. Accepted: May 19, 2023. Available online: May 23, 2023
https://doi.org/10.1590/1679-78257514

1 INTRODUCTION

Piles and pile groups are a common choice of foundations for heavy structures such as buildings, bridges, and wind turbine towers. They work by locally increasing the stiffness of the soil, which improves its ability to support the structure safely, while using a relatively small amount of material.

Some of the first descriptions of pile behavior were put forward by Poulos and Aust (1968), Poulos and Mattes (1971), Poulos (1971), Butterfield and Banerjee (1971) and Banerjee (1978) for the static case, who described the interaction between embedded elastic piles and their surrounding soil via a combination of Mindlin's fundamental solution for the soil part and differential equilibrium equations for the piles part. Coupling between the body of the pile and the bulk of the soil were obtained by imposing equilibrium and continuity conditions at their interface. A Winkler type of model, which describes the soil as sets of concentrated or distributed springs and dashpots, has been used by other authors to represent nonlinearity, ihnomogeneity, and dynamic pile behaviors (Penzien, 1970; Matlock, 1970; Prakash and Chandrasekaran, 1973; Desai and Kuppusamy, 1980). Winkler models, however, are incapable of representing the interaction between piles, among other difficulties (Sen et al., 1985). Lysmer (1970) and Lysmer and Waas (1972) introduced a layer stiffness approach to overcome the limitations of the Winkler models. Novak (1974) and Nogami and Novák (1976) proposed a continuous pile–soil model that is able to account for energy exchanged between pile and soil. A finite element scheme has been used by Wolf and von Arx (1978) and Waas and Hartmann (1981) to obtain pile and soil influence functions and then use them to compute the dynamic impedance of embedded piles. Kausel and Peek (1982) proposed the semi-discrete thin layer method, which uses a rigorous formulation for waves in layered media to describe dynamic pile behavior. Their method consists of the linearization of the transcendental Green's functions that describe each soil layer, so that the effect of these functions in a multilayered soil system can be superposed algebraically. A similar idea had been used in the impedance matrix method (Kausel and Roësset, 1981) to consider layers of arbitrary thickness and higher frequencies of excitation. Later, Kaynia and Kausel (1991) extended the impedance matrix method to describe pile–soil interaction via a finite–boundary element coupling scheme. In their solution, the piles are modeled as finite beam elements, and their surrounding soil layer is modeled as a series of stacked buried ring loads, which can be seen as boundary elements of constant load distribution. Coupling between finite pile elements and boundary elements of soil was obtained by establishing direct equilibrium and compatibility conditions at their interface. The model proposed by Kaynia and Kausel (1991) can be used to compute the response of pile groups to external and seismic excitation, as well as the response of a rigid raft supported by pile groups. However, it cannot be used to compute the response of arbitraly-shaped and/or elastic structures supported by pile groups. Barros, Labaki and Mesquita (2019) and Labaki, Barros and Mesquita (2019, 2021) are some of the few models of elastic structures supported by piles that correctly account for the dynamic pile–soil interaction. These, however, are limited in that the structure that they consider are simple circular plates and that they consider a single pile. Additionally, a literature review on experimental analyses on the response of pile groups can be found in Loveridge et al. (2020), Rathod et al. (2020), and the references therein.

This paper presents a model of the time-harmonic response of piled structures, i.e., structures the foundation of which consists of a group of embedded piles. In this model, a finite element discretization is used to describe the response of the structure, which is coupled with the response of the embedded pile group obtained via the impedance matrix method. The paper brings original numerical results on the response of selected problems in which an accurate description of the response of the structure depends on properly modeling the interaction between piles through the soil.

1.1 Statement of the problem

Consider one or more arbitrarily-shaped, linear-elastic, three-dimensional structures. The structure is subjected to arbitrary, time-harmonic external loads of circular frequency ω, which can be concentrated or distributed, and applied at any point or surface of the structure. The structure is supported at discrete points by an arbitrary number of arbitrarily-positioned, linear-elastic, vertical cylindrical piles of length L and diameter d. The piles are embedded in a linear-elastic, isotropic, layered, three-dimensional half-space, representing the soil (Figure 1). The problem consists in determining the dynamic response of the structure to the external load. In this paper, the dynamic response of the structure is expressed in terms of the displacement of a selected point.

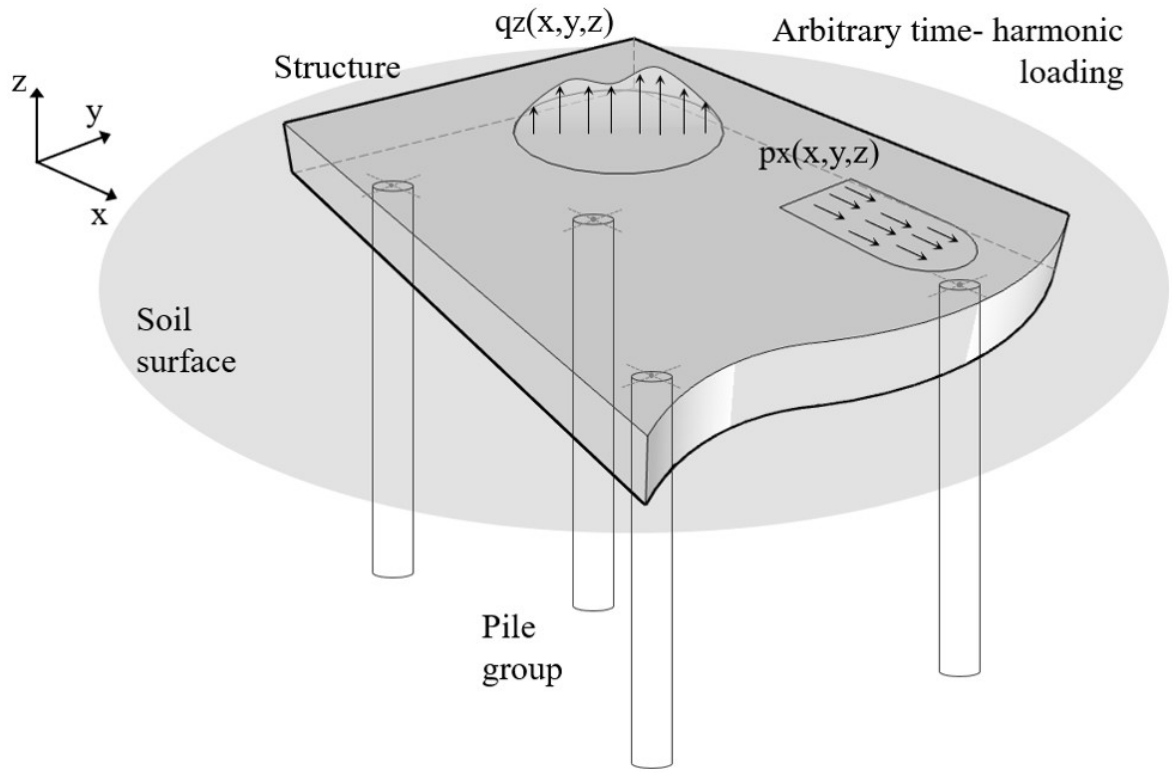

Figure 1. Arbitrarily-shaped structure supported by pile group considered in this paper.

2 FORMULATION OF THE MODEL

In this paper, a combination of coupled methods is used to describe the response of the piled structure. The first coupling is that of finite beam elements to describe the elastic piles in the pile group, together with boundary elements to describe their embedment in the surrounding soil. The second coupling is that of solid finite elements to describe the structure, together with the pile group coupling.

The structure is modeled via a finite element discretization, using three-dimensional, linear elastic, hexahedral finite elements with three translational degrees of freedom in each of its eight nodes. The stiffness and mass matrices of these elements are given by

$$\boldsymbol{k_e} = \int_{V_e} \boldsymbol{B^T D B} dV = \int_{-1}^{1}\int_{-1}^{1}\int_{-1}^{1} \boldsymbol{B^T D B} det(J) d\xi d\eta d\zeta \tag{1}$$

$$\boldsymbol{m_e} = \int_{V_e} \boldsymbol{\rho N^T N} dV = \int_{-1}^{1}\int_{-1}^{1}\int_{-1}^{1} \boldsymbol{\rho N^T N} det(J) d\xi d\eta d\zeta \tag{2}$$

in which $\boldsymbol{V_e}$ is the volume of the element, $\boldsymbol{D}$ is the constitutive matrix, $\boldsymbol{J}$ is the Jacobian of the transformation between the domains (x, y, z) and (ξ, η, ζ), and $\boldsymbol{N}$ and $\boldsymbol{B}$ are the vector of shape functions and the matrix of their derivatives (Cook, 2007). Following the classical assembly procedure, $\boldsymbol{k_e}$ and $\boldsymbol{m_e}$ are assembled into the global stiffness and mass matrices $\boldsymbol{K_S^G}$ and $\boldsymbol{M_S^G}$ of the structure. The equation of motion of the structure is $\boldsymbol{P}_S = \boldsymbol{K}_S \boldsymbol{U}_S$, in which $\boldsymbol{P}_S$ and $\boldsymbol{U}_S$ are respectively the vector of nodal forces and displacements, and

$$\boldsymbol{K}_S = \boldsymbol{K_S^G} - \boldsymbol{\omega^2 M_S^G} \tag{3}$$

is the dynamic global stiffness matrix of the structure (Petyt, 2015).

The pile group model used in this paper is the impedance matrix method (Kaynia and Kausel, 1991). The traction distribution at the pile–soil interface is approximated by two orthogonal horizontal components and one frictional component in the vertical direction. The interface is discretized into a number of segments, in each of which the traction distribution components are assumed to be uniformly distributed. The traction distribution at the pile tip is assumed to be uniformly distributed on that interface as well. The body of the pile is discretized into a number of one-dimensional

finite beam elements. Traction–displacement relations at the soil segments along each pile element are obtained via soil influence functions corresponding to buried cylindrical loads (Barros et al, 2019). The fully-bonded condition is assumed at the pile–soil interface, which is expressed as strict continuity and equilibrium conditions at that interface. The equation of motion for the embedded pile group resulting from this model is $\boldsymbol{P}_p = \boldsymbol{K}_p \boldsymbol{U}_p$, in which $\boldsymbol{P}_p$ is the vector of forces and moments at the ends of the piles, $\boldsymbol{U}_p$ is the vector of resulting displacements and rotations at the ends of the piles, and

$$\boldsymbol{K}_p = \boldsymbol{K}_f + \boldsymbol{\Psi}(\boldsymbol{F}_s + \boldsymbol{F}_p)^{-1}\boldsymbol{\Psi} \tag{4}$$

is the stiffness matrix of the embedded pile group, in which $\boldsymbol{K}_f$ is the stiffness matrix of the body of the piles in the group, $\boldsymbol{\Psi}$ is the stiffness matrix of embedded piles considering clamped-end conditions, and $\boldsymbol{F}_p$ and $\boldsymbol{F}_s$ are the flexibility matrices of the piles and soil. The reader may refer to Kaynia and Kausel (1991) for a detailed description of the terms involved in Equation 4.

The equilibrium equation for the piled structure is obtained by coupling the response of the structure with that of the embedded pile group. This is achieved by imposing continuity and equilibrium conditions between the pile heads, as discrete points, and the nodes of the mesh of the structure to which each pile head is connected. The resulting equation of motion is given by $\boldsymbol{P} = \boldsymbol{K}\boldsymbol{U}$, in which $\boldsymbol{P}$ and $\boldsymbol{U}$ are vector of nodal forces and displacements of the structure, and

$$\boldsymbol{K} = \begin{bmatrix} K_{11}^s & \cdots & K_{1m}^s & \cdots & K_{1n}^s & \cdots & K_{1N}^s \\ \vdots & \ddots & \vdots & & \vdots & & \vdots \\ K_{m1}^s & \cdots & K_{mm}^s + K_{ii}^p & \cdots & K_{mn}^s + K_{ij}^p & \cdots & K_{mN}^s \\ \vdots & & \vdots & \ddots & \vdots & & \vdots \\ K_{n1}^s & \cdots & K_{nm}^s + K_{ji}^p & \cdots & K_{nn}^s + K_{jj}^p & \cdots & K_{nN}^s \\ \vdots & & \vdots & & \vdots & \ddots & \vdots \\ K_{N1}^s & \cdots & K_{Nm}^s & \cdots & K_{Nn}^s & \cdots & K_{NN}^s \end{bmatrix} \tag{5}$$

is the dynamic impedance matrix of the coupled piled structure (Vasconcelos, 2019). Equation 5 shows an example in which the finite element mesh of the structure has *N* nodes, two of which (nodes *m* and *n*) are connected to pile heads (denoted by piles *i*, which is connected to node *m*, and *j*, which is connected to node *n*). Each of the terms in the matrix K corresponds to a 3 × 3 submatrix of $\boldsymbol{K}_s$ and $\boldsymbol{K}_p$, denoted by the superindexes s and p respectively. The submatrices of $\boldsymbol{K}_s$ that correspond to nodes of the structure that are connected to pile heads (nodes *m* and *n*) are superposed with submatrices of $\boldsymbol{K}_p$, corresponding to the stiffness of the pile head that is connected to that node. Note that ${K_{mm}}^s$ and ${K_{nn}}^s$ are superposed with ${K_{ii}}^p$ and ${K_{jj}}^p$, respectively, which denotes the fact that the stiffness of nodes *m* and *n* are affected by the flexibility of the piles to which they are connected. However, note also that ${K_{mn}}^s$ is superposed with ${K_{ij}}^p$ and ${K_{nm}}^s$ is superposed with ${K_{ji}}^p$. This corresponds to the cross influence between piles *i* and *j* through the soil, and well as to their influence on nodes *m* and *n*, which are properly accounted for in this model.

3 NUMERICAL RESULTS

The model presented in this article was used to compute the response of selected problems of interest in engineering practice, namely, the problem of a wind turbine tower and the problem of foundation blocks. This section also presents results on the response of structures that interact with each other through the soil. The material properties of concrete ($\mathrm{E} = 21.5\mathrm{GPa};\ \nu = 0.2;\ \rho = 2500\mathrm{kg}/\mathrm{m}^3$) and steel ($\mathrm{E} = 200\mathrm{GPa};\ \nu = 0.3;\ \rho = 7850\mathrm{kg}/\mathrm{m}^3$) typically used in practice are considered in these analyses. The material properties considered for the soil are described in each case. The results are presented in terms of the normalized displacements $u_{ij} = U_{ij}/F_j$, in which U_{ij} expresses displacements in the i – direction due to time-harmonic loads applied in the j – direction $(i, j = x, z)$ and of the normalized frequency of excitation $\mathrm{a}_0 = \omega \mathrm{d} / \mathrm{c}_\mathrm{s}$, in which c_s is the shear wave speed of soil.

3.1 Wind turbine tower

This section considers the response of the wind turbine tower sketched in Figure 2. The tower is modeled as a 78m-tall cylindrical steel tower, supported by a conical concrete base with 14m of diameter. The structure is supported by a group of eighteen 10.8m-long concrete piles with 0.7m diameter, uniformly distributed in a circle of 12.5m diameter from the center of the tower. The tower was discretized in 5724 finite elements. Time-harmonic horizontal (x – direction, F_x) and vertical (z – direction, F_z) loads are uniformly distributed on the top surface of the tower. The results are

presented in terms of the normalized displacements calculated at the point of coordinates x = 2.57m; z = 80.75m, at the outer rim of the top surface of the tower. The results compare three modeling assumptions that one can find in engineering practice. Case 1 corresponds to the case in which the entire bottom of the tower is assumed to be fixed. This is obtained by imposing a zero-displacement condition in all nodes of the bottom surface of the tower. Case 2 corresponds to the case in which only the 18 points where the piles are installed are assumed as fixed. That is, Cases 1 and 2 consider no interaction between the structure and the soil. Case 3 is that in which the interaction between the tower and its supporting pile group foundation is modeled properly: the flexibility of the piles and the energy exchanged between them through the soil is properly accounted for. No displacement boundary condition is imposed in this case. The soil considered in Case 3 is a homogeneous soil with $\mathrm{E} = 21.5\mathrm{MPa}$, $\nu = 0.4$, and $\rho = 1250\mathrm{kg/m^3}$.

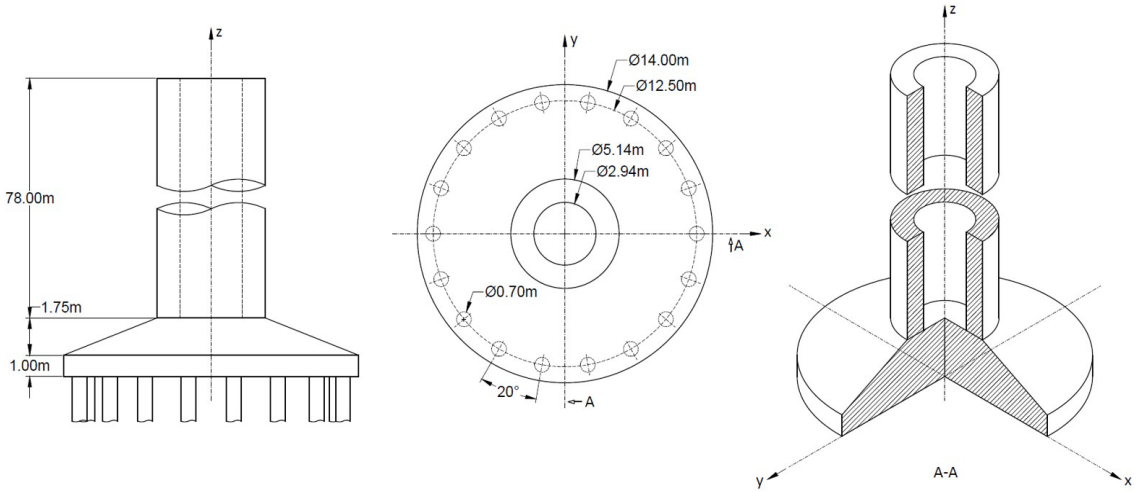

Figure 2 Geometry of the wind turbine tower considered in this section.

Figures 3 to 6 show the response of the tower in the three cases. These results show that the resonant frequencies of the tower in the horizontal excitation case in Case 2 are slightly lower than those in Case 1. This is physically consistent, since the model in which the entire base of the tower is considered to be fixed is more rigid, which corresponds to a model with higher natural frequencies, than that in which only a few points are fixed. The difference between Cases 1 and 2 is more pronounced in the vertical direction than in the horizontal direction, due to the arrangement of the piles in a circle, which allows for more flexibility of the base of the tower in the vertical direction. However, the most outstanding difference in these results is between Cases 1 and 2 and Case 3. In Case 3, not only the natural frequencies of the system are altered significantly, but the amplitude of the response is considerably attenuated. This is due to the geometric damping characteristics of the soil. Taking into account the effect of the soil in the design of the tower corresponds to adding a strong damper into the system, which is otherwise purely elastic in Cases 1 and 2.

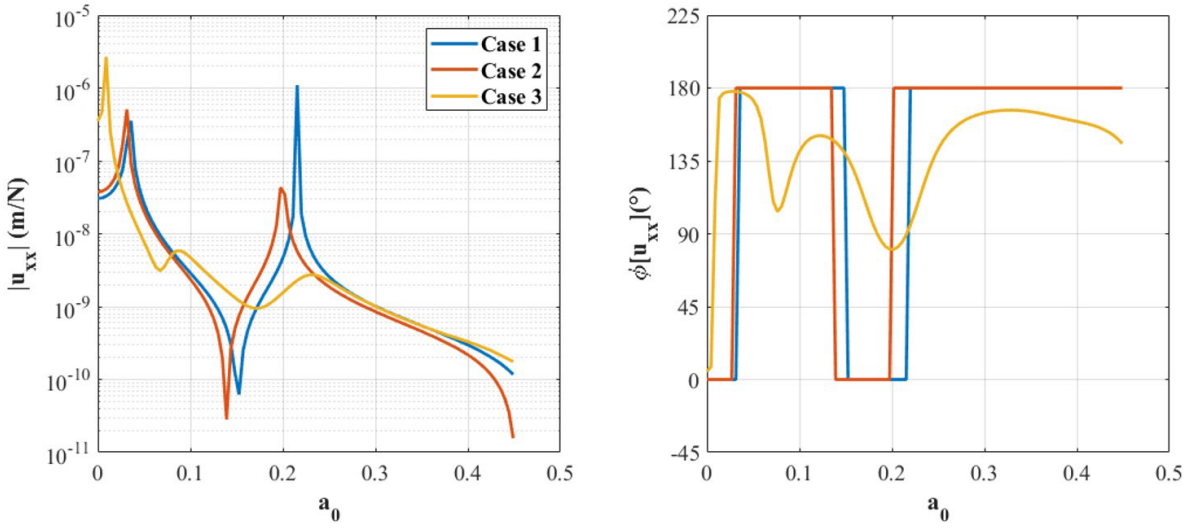

Figure 3 Horizontal response of the tower due to horizontal loads.

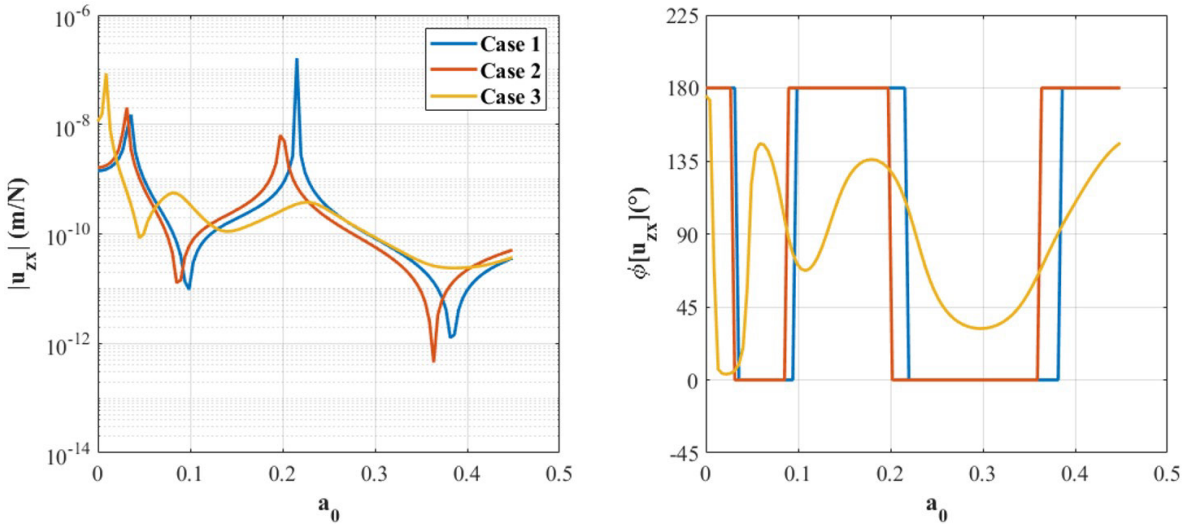

Figure 4 Vertical response of the tower due to horizontal loads.

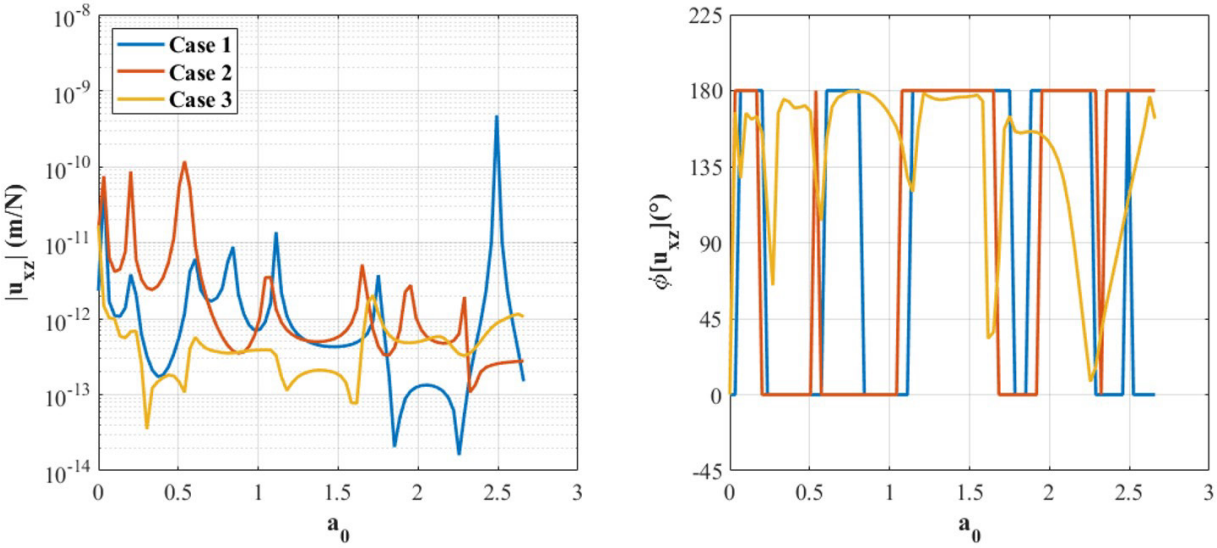

Figure 5 Horizontal response of the tower due to vertical loads.

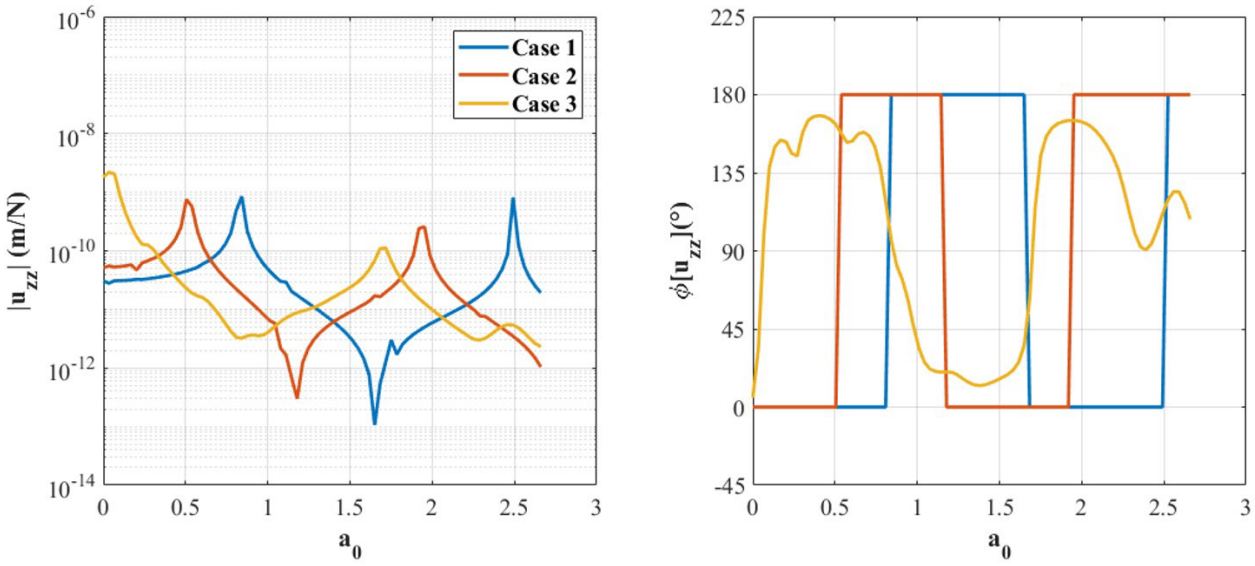

Figure 6 Vertical response of the tower due to vertical loads.

3.2 Foundation blocks

This section considers the response of the three designs for foundation blocks shown in Figure 7. Foundation blocks are routinely used in the design of bridges and buildings. Concrete is used for the blocks and their supporting piles in all analyses in this section. For the blocks with two, three and four piles, are used finite element meshes with 160, 240 and 400 elements, respectively. The properties of a layered soil found in engineering practice have been considered in this analysis (Garcia and Albuquerque, 2019). The thickness and material properties of each layer are given in Table 1. The blocks are subjected to horizontal and vertical time-harmonic loads that are uniformly distributed over their top surface. Their response is presented in terms of the normalized displacement of the center of the top surface of the blocks and of the normalized frequency of excitation $a_0 = \omega d / c_s$, in which $c_s = 55.8 m/s$ is the shear wave speed in the top layer of soil.

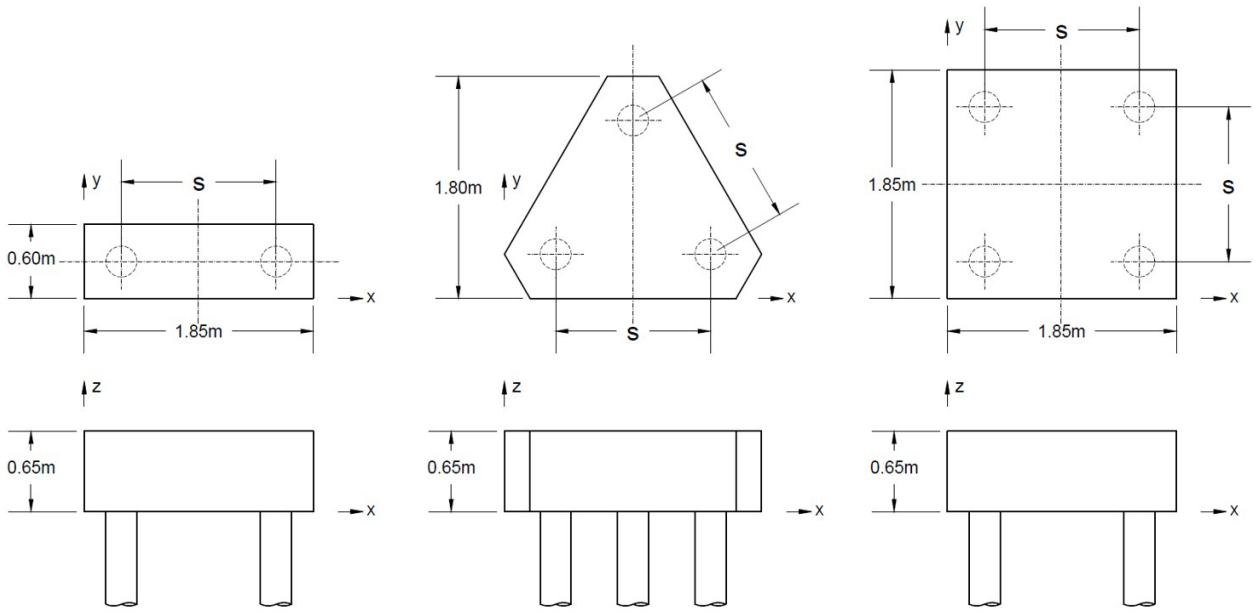

Figure 7 Geometry of the foundation blocks considered in this section.

Table 1 Dimensions and material properties of the soil layers used in this analysis

Material	*h* (m)	*E* (MPa)	*v*	*ρ* (kg / m^3)
Silty-sandy clay	1.35	12.6	0.4	1447.5
Silty sand	6	12	0.4	1529
Sandy-clayey silt	4	11	0.4	1549.5
Impenetrable layer	∞	100	0.3	2038.7

Figures 8 to 13 show the influence of pile length in the response of the three foundation blocks. All results consider a pile distance s = 5d. The results show that the three foundation blocks present similar dynamic responses, with displacement maxima at comparable frequencies of excitation. A small difference is observed in the amplitude of the response, in that the more piles are used in the foundation block, the lower the overall amplitude of its response. The amplitude of motion in all cases is larger in the horizontal direction, associated with the more flexible, bending behavior of the piles, than in the vertical direction, associated with the compressional behavior of the piles. In the vertical response cases, an increase in pile length corresponds to a reduced overall response, which is due to the load transfer from the pile to the soil throughout its increased length. In the horizontal case, however, increasing the length of the pile has generally a marginal effect on the response of the system. This is because the bending moment along the body of the pile resulting from horizontal loadings at the pile head is reduced for larger depths of embedment (Labaki et al., 2019). More deeply embedded portions of the body of the pile contribute increasingly less to the horizontal response of the pile.

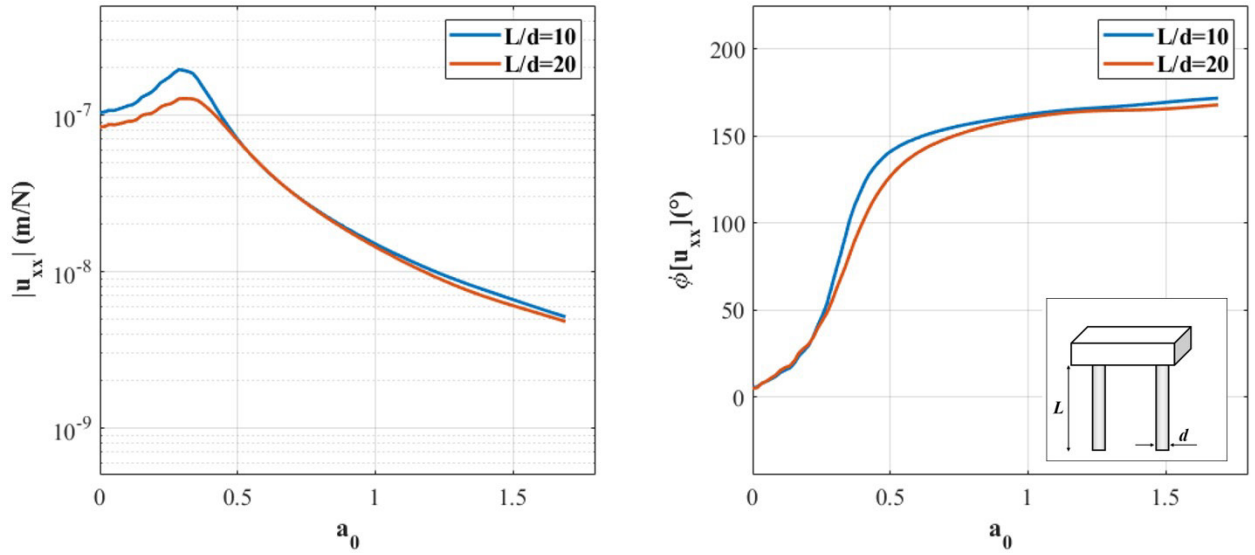

Figure 8 Influence of pile length in the horizontal response of the narrow foundation block.

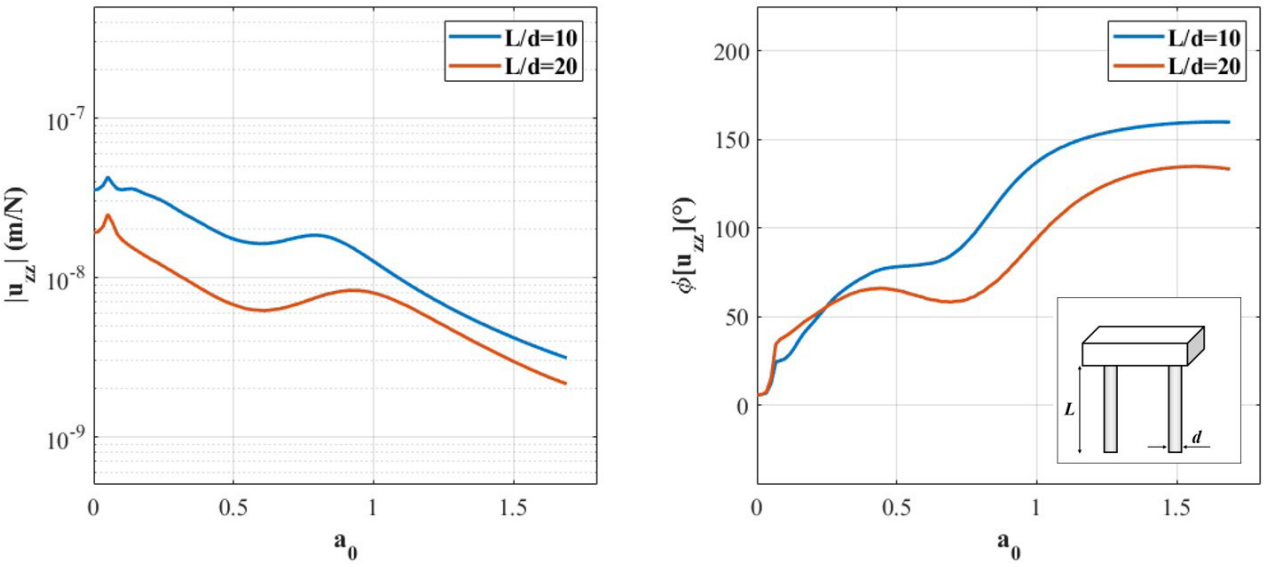

Figure 9 Influence of pile length in the vertical response of the narrow foundation block.

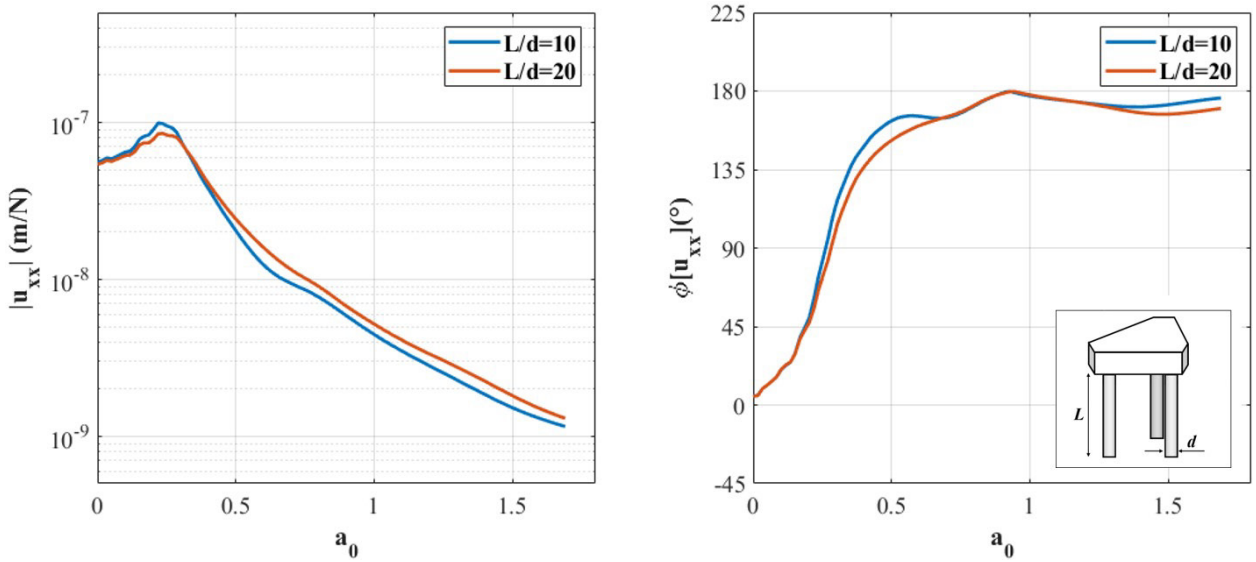

Figure 10 Influence of pile length in the horizontal response of the triangular foundation block.

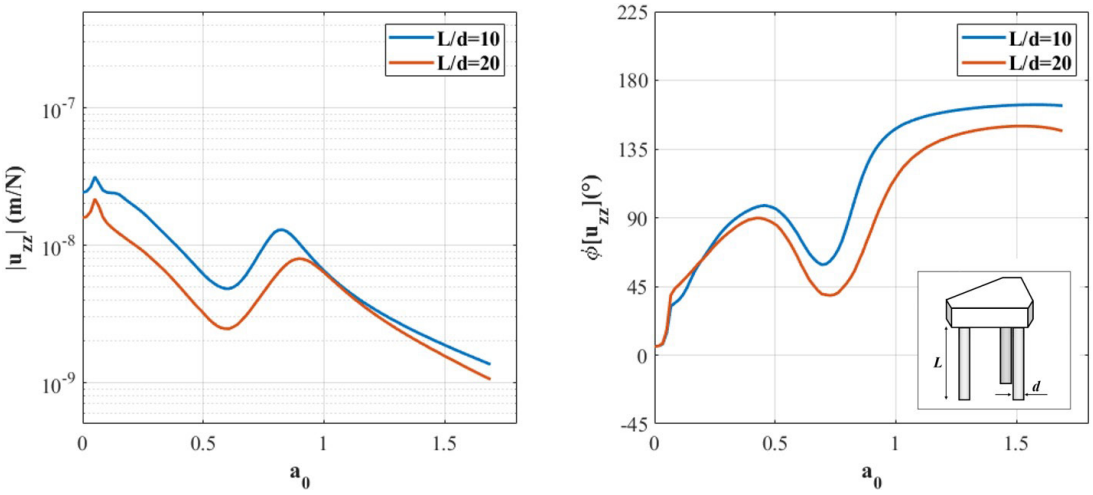

Figure 11 Influence of pile length in the vertical response of the triangular foundation block.

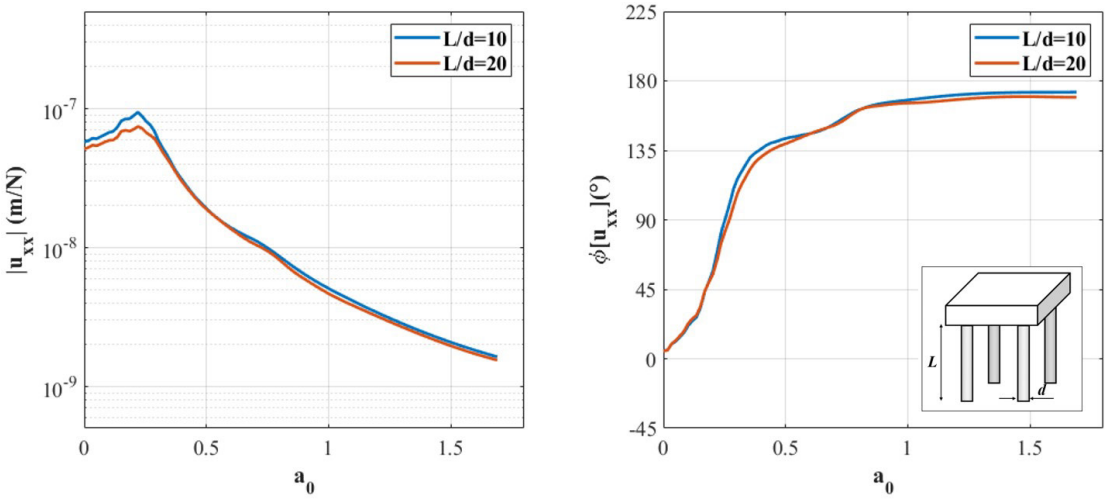

Figure 12 Influence of pile length in the horizontal response of the square foundation block.

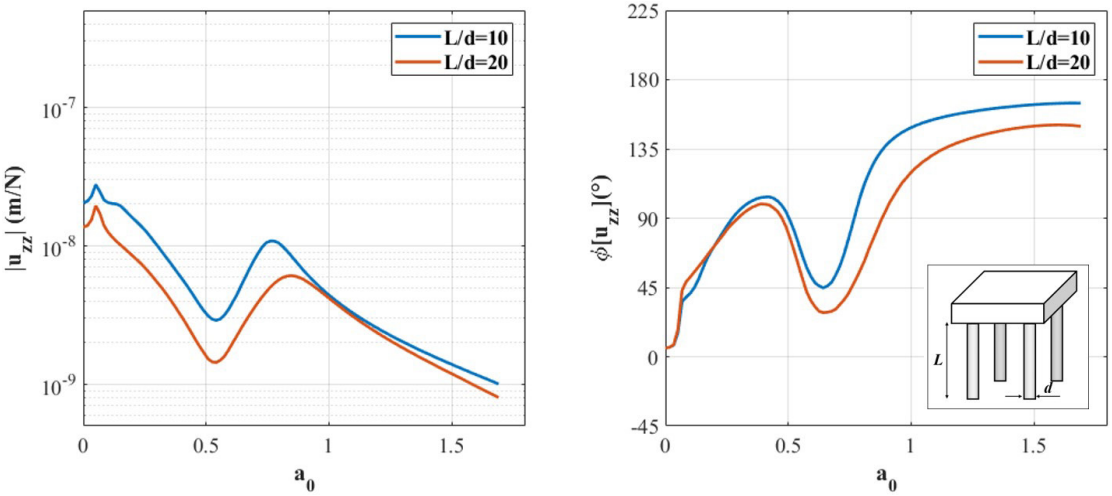

Figure 13 Influence of pile length in the vertical response of the square foundation block.

Figures 14 to 19 show the influence of pile distance in the response of the three foundation blocks. Two cases were considered, s = 3d and s = 5d, which differ in that the closer together the piles are, the more they affect each other's response (Poulos and Davis, 1980). All cases consider pile length L = 10d. The results show that the pile distances considered in this case have little influence in the horizontal response of the foundation blocks. The most significant influence of pile distance is observed in the vertical case. There is no clear trend on the influence of the two pile distance

cases in the vertical response of the foundation blocks: increasing pile distance from s = 3d to s = 5d affects the response of the blocks in no predictable pattern. This vouches for the importance of analyzing each design case individually, with models that can account for pile interaction, such as the one presented in this article.

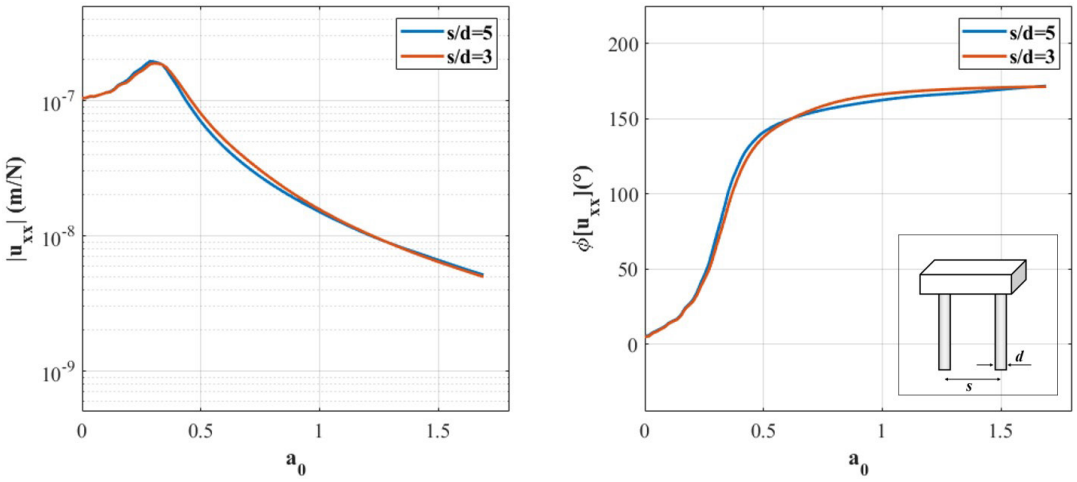

Figure 14 Influence of pile distance in the horizontal response of the narrow foundation block.

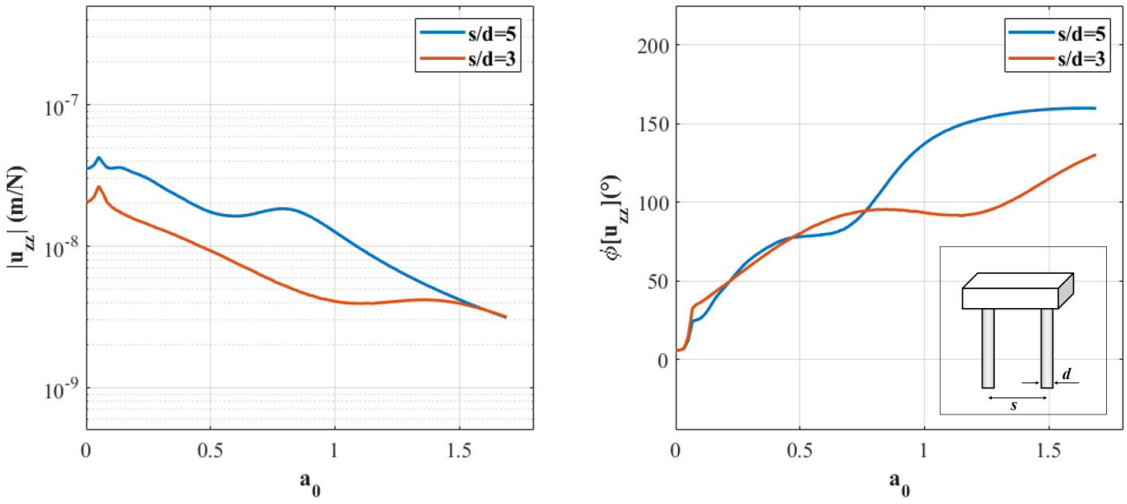

Figure 15 Influence of pile distance in the vertical response of the narrow foundation block.

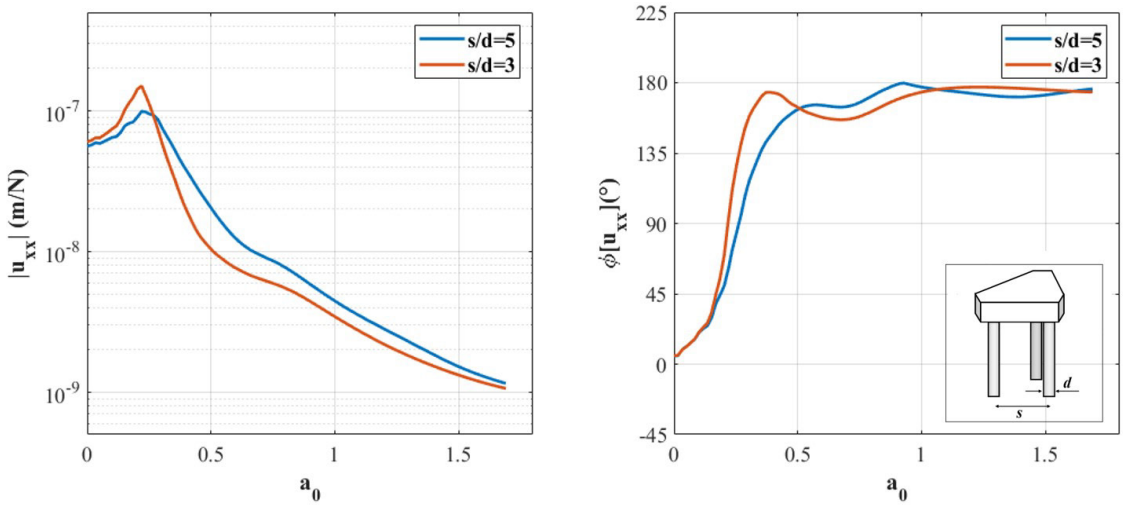

Figure 16 Influence of pile distance in the horizontal response of the triangular foundation block.

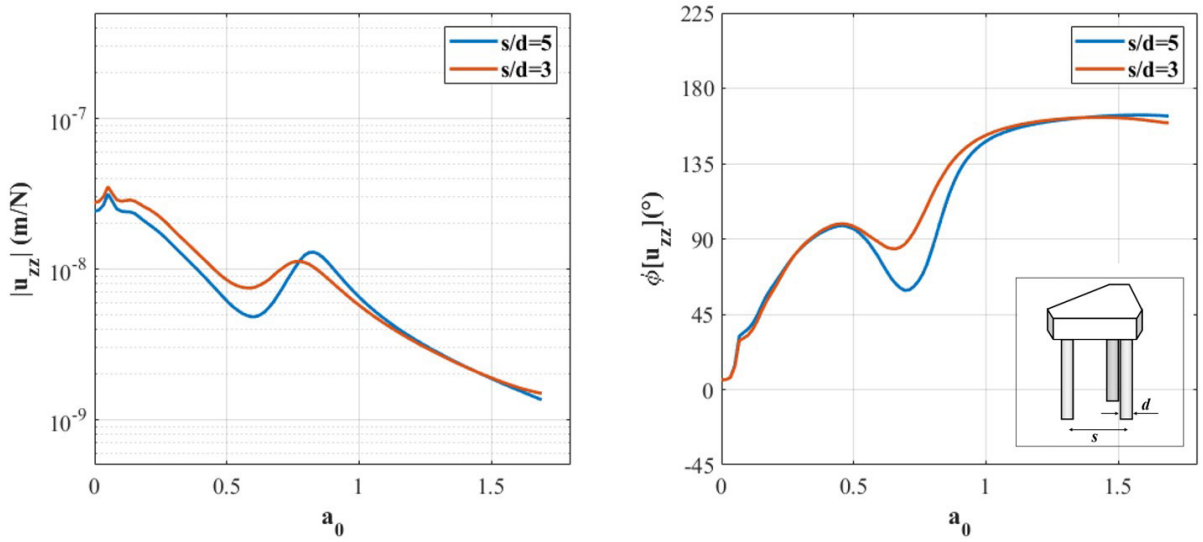

Figure 17 Influence of pile distance in the vertical response of the triangular foundation block.

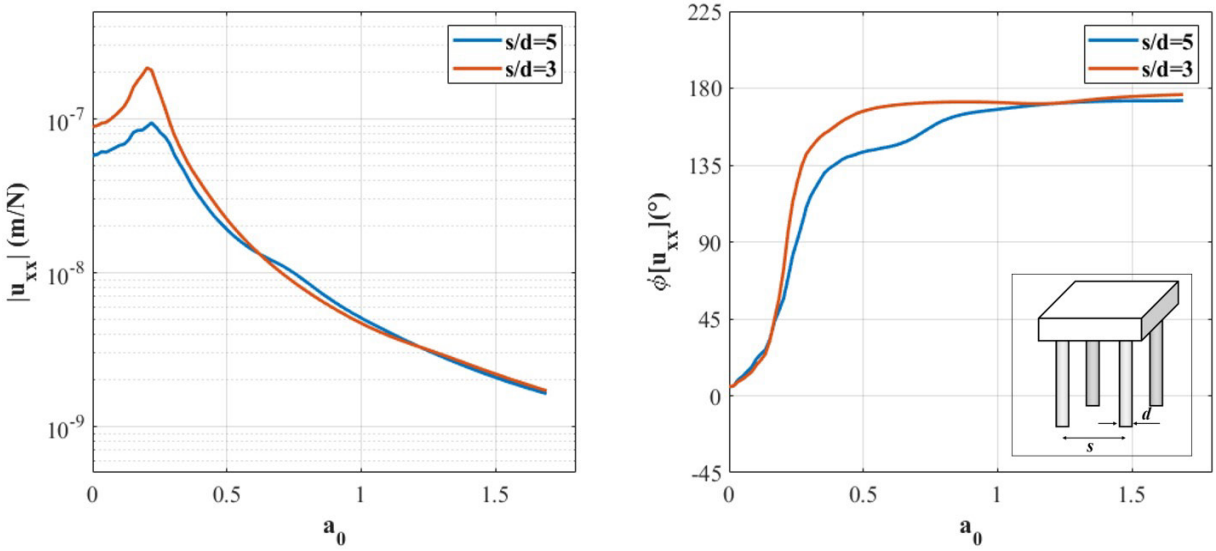

Figure 18 Influence of pile distance in the horizontal response of the square foundation block.

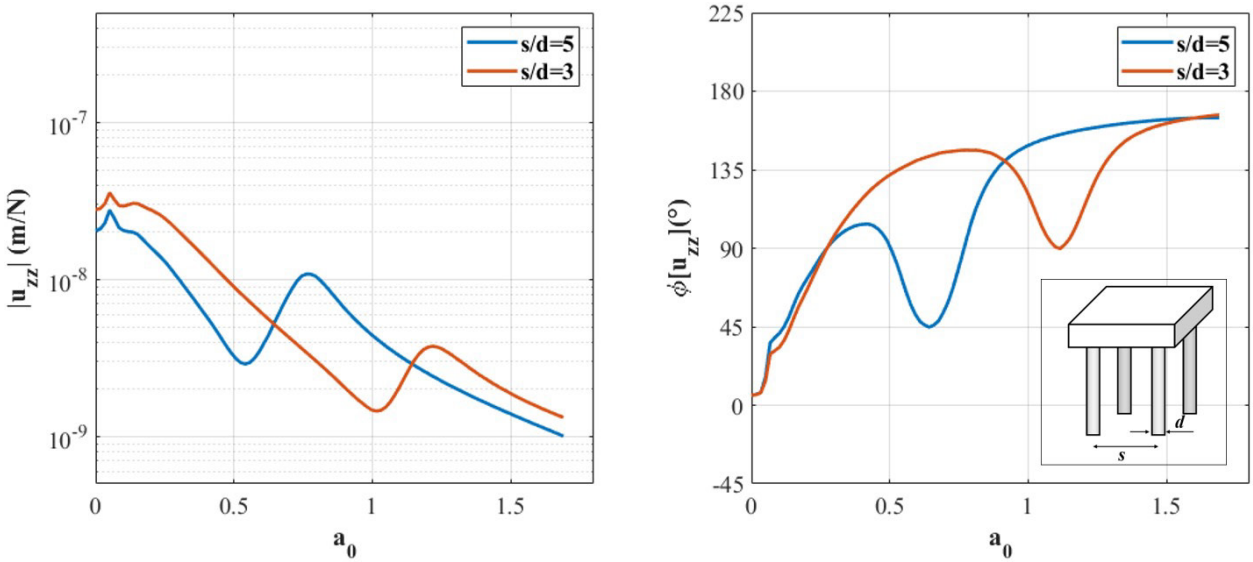

Figure 19 Influence of pile distance in the vertical response of the square foundation block.

3.3 Structure–soil–structure interaction

This section considers a representative problem of practical engineering interest in which piled structures are separated from each other, but interact because of the energy that propagates from one to the other through the soil (Figure 20). In this case, a piled concrete raft is subjected to horizontal and vertical time-harmonic loads that are uniformly distributed over its top surface. The effect of this loading is calculated at points A and B, at the center of the bottom and top surfaces of a piled concrete tower, that is separated from the raft by a center-to-center distance S. The raft and tower have square cross sections of sides s=2.5m and height h=1.0m and H, respectively. Both the raft and the tower are supported by four concrete piles of diameter d = 0.4m and length L = 15m, placed at each of their four bottom corners. The raft and the tower are modeled by 400 and $24(H/d)$ finite elements, respectively. A homogeneous soil with properties $c_s = 250\text{m/s}, \nu = 0.4$ and $\rho = 1600\text{kg/m}^3$ is considered. The results are presented in terms of the normalized displacement of points A and B.

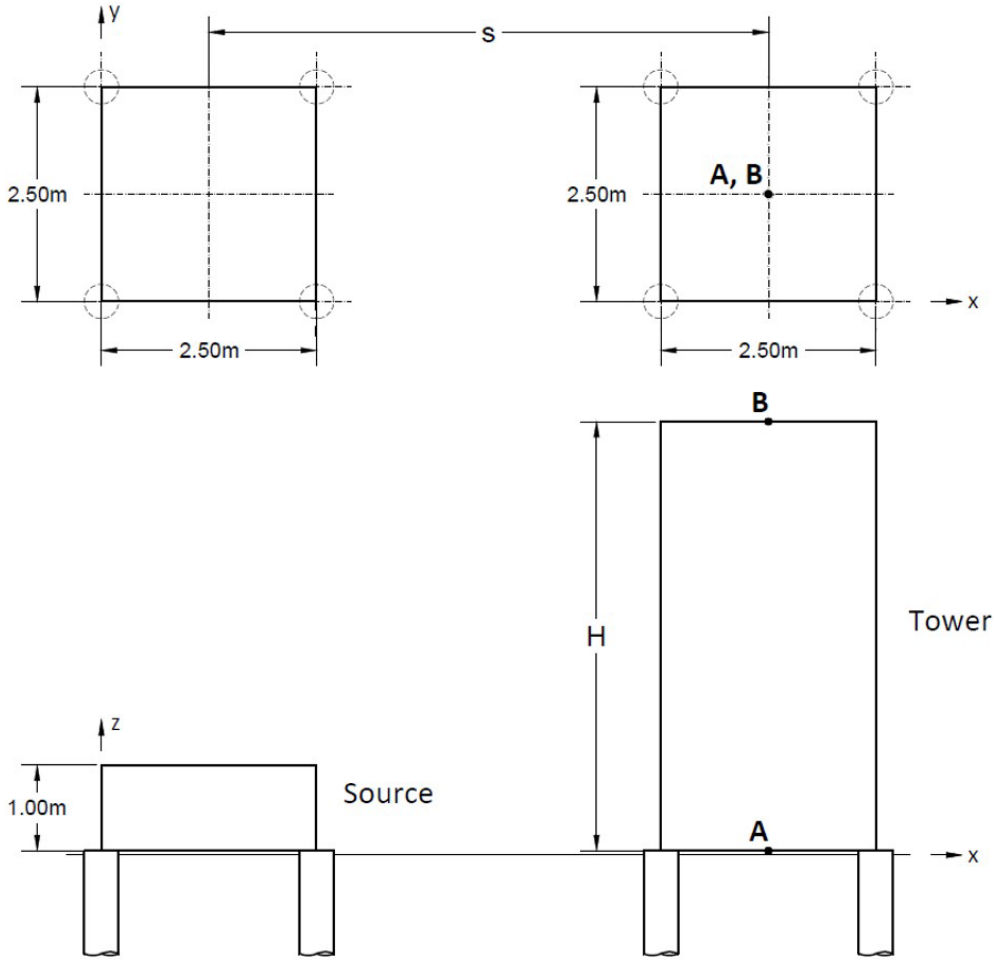

Figure 20 Geometry of the piled raft and piled tower considered in this case.

Figures 21 to 24 show the effect of the height H of the tower in its response. All cases consider S = 20d. These results show that increasing the height of the tower results in lower resonant frequencies in its horizontal response, regardless of the loading direction. This is physically consistent, since taller towers behave as longer beams, in terms of their horizontal response, which have lower natural frequencies. The same is observed for both the top and bottom of the tower, although the magnitude of vibration of the bottom of the tower is about two orders of magnitude lower than that of the top of the tower, as expected. The vertical response of the tower, on the other hand, is less significantly affected by its height, regardless of the loading direction. Increasing the height of the tower results in a reduction of its overall magnitude of vibration in the vertical direction. The vertical response of the tower is primarily governed by the compressional modes of the tower, which is much stiffer in compression than in bending. This increased stiffness in the vertical direction causes the top and bottom of the tower to move in tandem, and is also reflected in the fact that the resonant frequencies of the system are much higher in the vertical direction, and in the fact that the magnitude of vertical vibration is about two orders of magnitude lower than those of horizontal vibration, regardless of the loading direction.

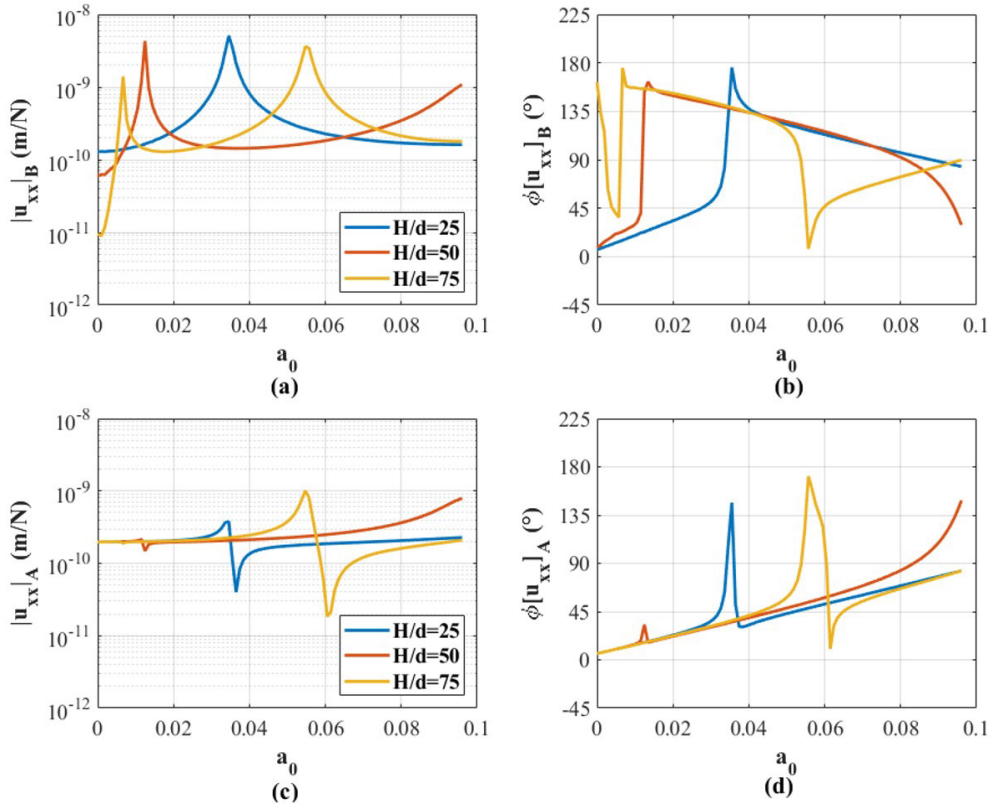

Figure 21 Influence of the height of the tower in its horizontal response due to horizontal loads applied at the raft. Parts (a) and (b) show the magnitude and phase of the vibration of point B, at the top of the tower. Parts (c) and (d) show the magnitude and phase of the vibration of point A, at the bottom of the tower.

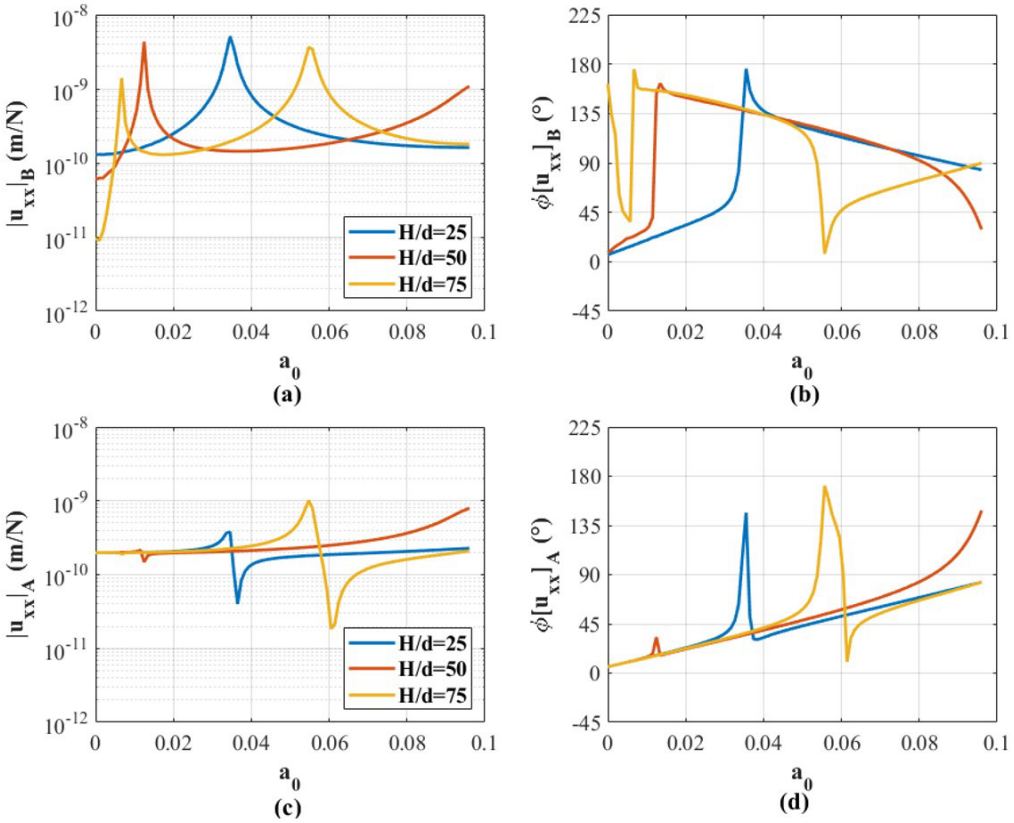

Figure 22 Influence of the height of the tower in its vertical response due to horizontal loads applied at the raft. Parts (a) and (b) show the magnitude and phase of the vibration of point B, at the top of the tower. Parts (c) and (d) show the magnitude and phase of the vibration of point A, at the bottom of the tower.

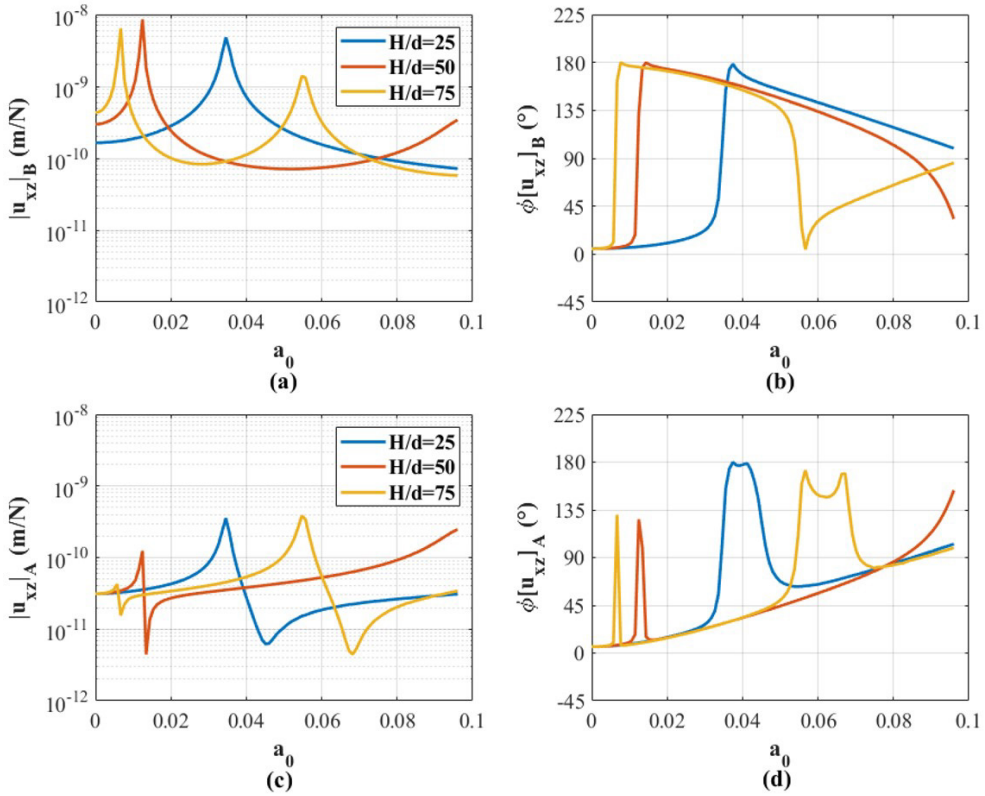

Figure 23 Influence of the height of the tower in its horizontal response due to vertical loads applied at the raft. Parts (a) and (b) show the magnitude and phase of the vibration of point B, at the top of the tower. Parts (c) and (d) show the magnitude and phase of the vibration of point A, at the bottom of the tower.

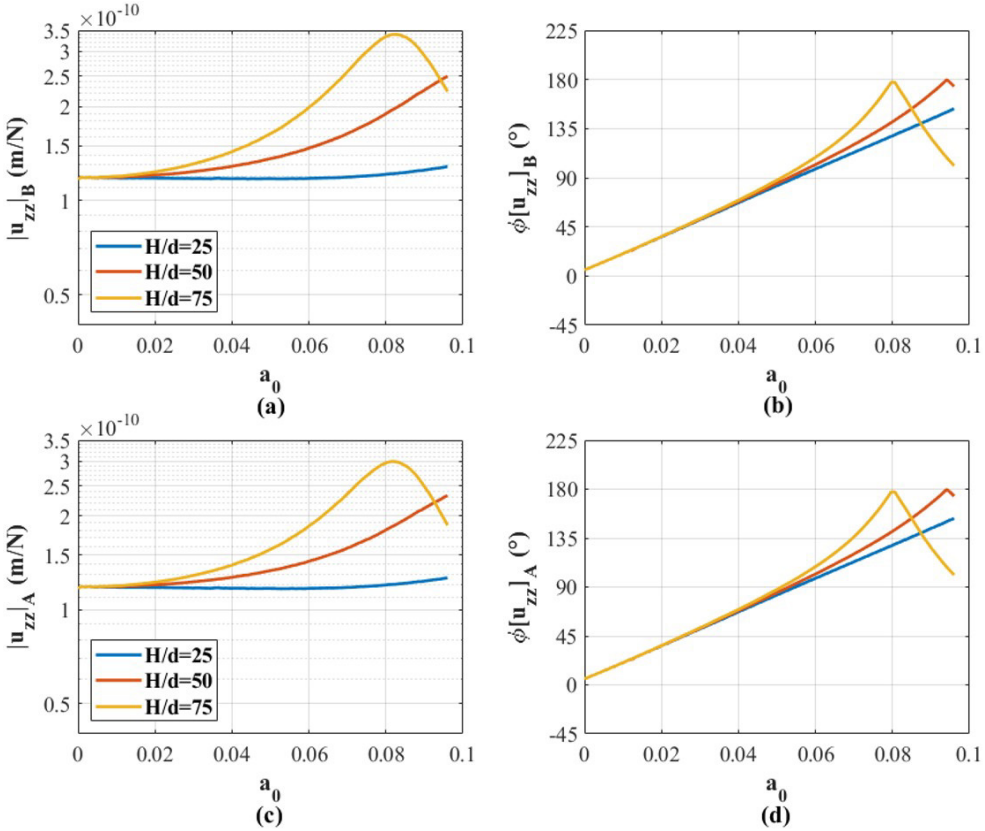

Figure 24 Influence of the height of the tower in its vertical response due to vertical loads applied at the raft. Parts (a) and (b) show the magnitude and phase of the vibration of point B, at the top of the tower. Parts (c) and (d) show the magnitude and phase of the vibration of point A, at the bottom of the tower.

Figures 25 and 26 show the influence of the raft-to-tower distance S in the response of the system. For the sake of brevity, only the direct responses u_{xx} and u_{zz} are shown, since they are sufficient to illustrate the influence of S in this problem. All cases consider H = 50d. These results show that the influence of *S* in the response of the system is merely the attenuation of the magnitude of vibration of the tower as it becomes more distant from the raft. This attenuation is consistent with the fact that the energy emanating from the raft is quickly dissipated as it travels through the soil, due to the strong geometric damping provided by the soil.

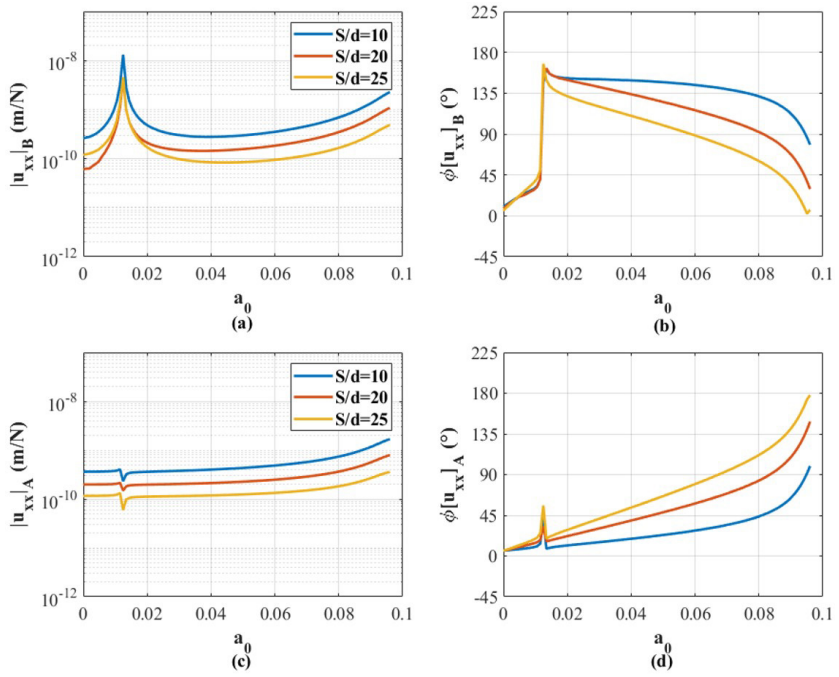

Figure 25 Influence of raft–tower distance in the horizontal response of the tower due to horizontal loads applied at the raft. Parts (a) and (b) show the magnitude and phase of the vibration of point B, at the top of the tower. Parts (c) and (d) show the magnitude and phase of the vibration of point A, at the bottom of the tower.

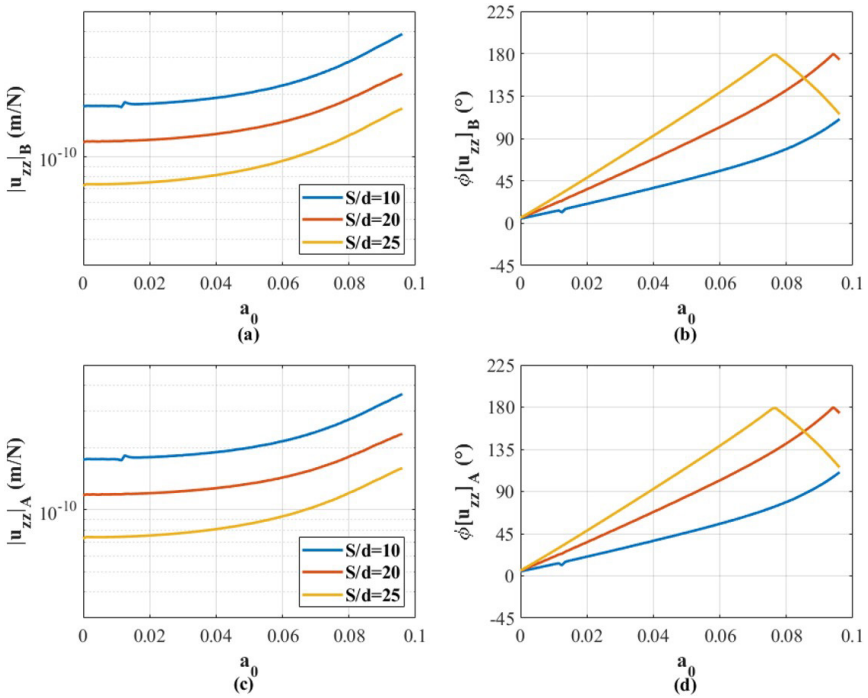

Figure 26 Influence of raft–tower distance in the vertical response of the tower due to vertical loads applied at the raft. Parts (a) and (b) show the magnitude and phase of the vibration of point B, at the top of the tower. Parts (c) and (d) show the magnitude and phase of the vibration of point A, at the bottom of the tower.

Figures 27 and 28 show the horizontal and vertical response of the top of the tower for loads applied directly onto the tower. The resonant frequencies of the tower in the previous raft–tower system, under seismic excitation, are the same as in this case. These results indicate that the main phenomena governing the response of the tower are the tower's own vibration modes, rather than properties of the soil or of the source of loading.

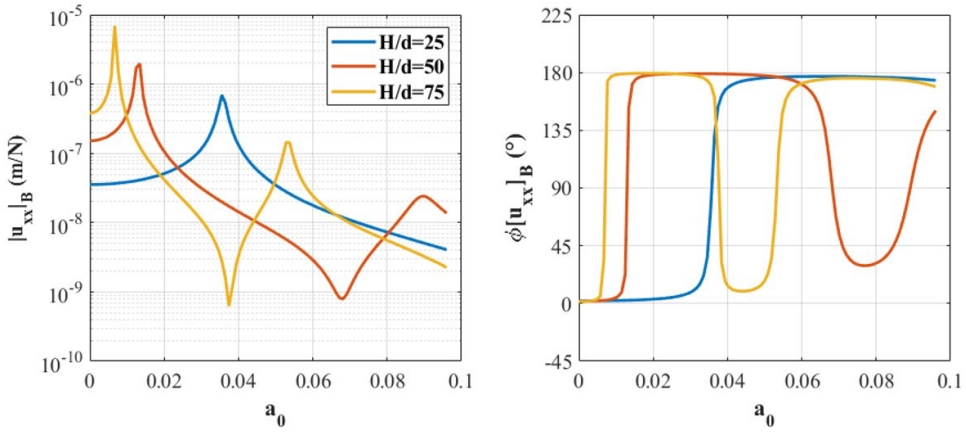

Figure 27 Influence of the height of the tower in its horizontal response due to horizontal loads applied directly on it.

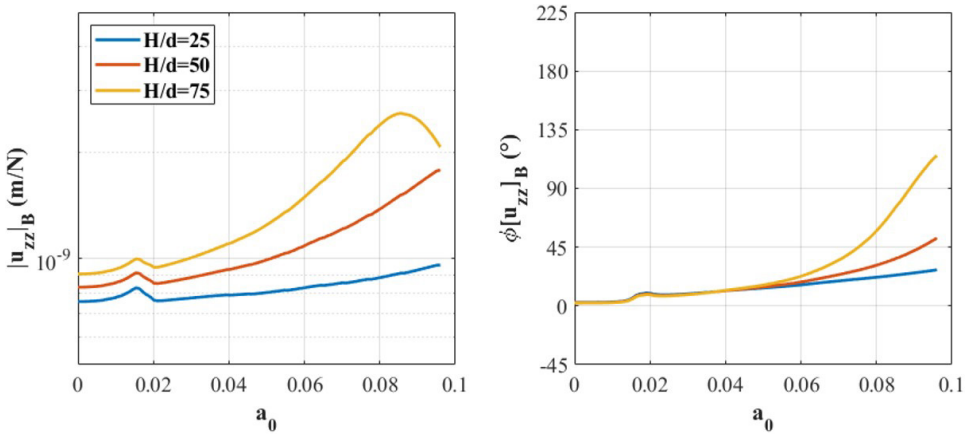

Figure 28 Influence of the height of the tower in its vertical response due to vertical loads applied directly on it.

4 CONCLUSIONS

This paper presented a model of the time-harmonic response of structures supported by groups of piles. A coupling scheme is used to represent the problem, in which finite elements of different types are used to model the structure and the piles, and their interaction with the soil is modeled via a boundary element discretization. The model is used to analyze selected problems of practical engineering interest. These include the case of a wind turbine tower in which three different approximations were used for its support, as well as the case of foundation blocks with three different designs. An analysis of structures that interact through the soil is also presented. The results show that the proposed model yields physically consistent results, and that approximations for the design of piled structures that disregard the flexibility of the soil and foundations may incur in significant misrepresentations of their behavior. In the wind turbine tower problem analyzed in this paper, for example, which has direct application in engineering practice, approximating the supports of the tower as rigid supports rather than flexible, energy-dissipating supports, incurs in an overestimation of the first natural frequency of the tower in 3.5 times in the horizontal direction of vibration, and 8.9 times in the vertical direction of vibration.

Acknowledgments

The research leading to this article has been funded in part by the São Paulo Research Foundation (Fapesp) through grant 2022/02753-5, by the Maranhão Research Foundation (Fapema) through grant 02120/19, and by the National Council for Scientific and Technological Development (CNPq), through grant 137111/2017-7.

Author's contributions: Formal analysis, AM Oliveira; Software, AM Oliveira; Writing – original draft, AM Oliveira; Methodology, ACA Vasconcelos; Software, ACA Vasconcelos; Writing – review & editing, ACA Vasconcelos; Conceptualization, J Labaki; Writing – review & editing, J Labaki; Supervision, J Labaki.

Editor: Marco L. Bittencourt and Josué Labaki

References

Banerjee, P. K. (1978). Analysis of axially and laterally loaded pile groups. Developments in Soil Mechanics 1:317–246.

Barros P., Labaki J., Mesquita E. (2019). IBEM-FEM model of a piled plate within a transversely isotropic half-space. Engineering Analysis with Boundary Elements 101:281–96.

Butterfield, R. and Banerjee, P. K. (1971). The elastic analysis of compressible piles and pile groups. Géotechnique 21(1):43–60.

Cook, R.D. (2007). Concepts and applications of finite element analysis, John Wiley and Sons.

Desai, C. S. and Kuppusamy, T. (1980). Application of a numerical procedure for laterally loaded structures, Numerical methods in offshore piling 93–99, Thomas Telford Publishing.

Garcia, J.R. and Albuquerque, P.J.R (2019). Analysis of the contribution of the block-soil contact in piled foundations, Latin American Journal of Solids and Structures 16(6).

Kausel, E. and Peek, R. (1982). Dynamic loads in the interior of a layered stratum: an explicit solution, Bulletin of the Seismological Society of America 72(5):1459–1481.

Kausel, E. and Roësset, J. M. (1981). Stiffness matrices for layered soils, Bulletin of the Seismological Society of America 71(6):1743–1761.

Kaynia, A. M. and Kausel, E. (1991). Dynamic of piles and pile groups in layered soil media, Soil Dynamics and Earthquake Engineering 10(8):386–401.

Labaki, J.; Barros, P. L. A.; Mesquita, E. (2021). A model of the time-harmonic torsional response of piled plates using an IBEM-FEM coupling, Engineering analysis with boundary elements 125: 241-249.

Labaki, J.; Barros, P. L. A.; Mesquita, E. (2019). Coupled horizontal and rocking vibration, and seismic shear-wave scattering of a piled plate on a transversely isotropic half-space, Engineering Analysis with Boundary Elements 106: 609-623.

Loveridge, F. and McCartney, J. S. and Narsilio, G. A. and Sanchez, M. (2020). Energy geostructures: a review of analysis approaches, in situ testing and model scale experiments, Geomechanics for Energy and the Environment 22: 100173.

Lysmer, J. (1970). Lumped mass method for rayleigh waves, Bulletin of the Seismological Society of America 60(1):89–104.

Lysmer, J. and Waas, G. (1972). Shear waves in plane infinite structures, Journal of Engineering Mechanics.

Matlock, H. (1970). Correlations for design of laterally loaded piles in soft clay, Offshore technology in civil engineering's hall of fame papers from the early years 77–94.

Nogami, T. and Novák, M. (1976). Soil-pile interaction in vertical vibration. Earthquake Engineering & Structural Dynamics 4(3):277–293.

Novak, M. (1974). Dynamic stiffness and damping of piles, Canadian Geotechnical Journal 11(4):574–598.

Penzien, J. (1970). Soil-pile foundation interaction, Earthquake engineering 11.

Petyt, M. (2015). Introduction to Finite Element Vibration Analysis, New York: Cambridge University Press.

Poulos, H. G. (1971). Behavior of laterally-loaded piles: II - pile groups, Journal of the Soil Mechanics and Foundation Division 97(SM5):733–751.

Poulos, H. G. and Aust, A. (1968). Analysis of the settlement of pile groups. Géotechnique 18(4):449–471.

Poulos, H.G. and Davis, E.H. (1980). Pile foundation analysis and design, Sydney: Rainbow-bridge book co.

Poulos, H. G. and Mattes, N. S. (1971). Settlement and load distribution analysis of pile groups. Australian Geomechanics Journal 1(1).

Prakash, S. and Chandrasekaran, V. (1973). Pile foundation under lateral dynamic loads, International Journal of Rock Mechanics and Mining Sciences & Geomechanics Abstracts, Pergamon.

Rathod, D. and Krishnanunni, K.T. and Nigitha, D. (2020). A review on conventional and innovative pile system for offshore wind turbines, Geotechnical and Geological Engineering 38(4): 3385-3402.

Sen, R., Kausel, E., and Banerjee, P. K. (1985). Dynamic analysis of piles and pile groups embedded in non-homogeneous soils, International Journal for Numerical and Analytical Methods in Geomechanic 9(6):507–524.

Vasconcelos, A. C. A. (2019). An impedance-matrix coupling scheme for arbitrarily-shaped structures supported by pile groups, University of Campinas.

Waas, G. and Hartmann, H. G. (1981). Impedance function of a group of vertical piles, Structural mechanics in reactor technology K.

Wolf, J. P. and von Arx, G. A. (1978). Impedance function of a group of vertical piles. In Proceedings of the Specialty Conference on Soil Dynamics and Earthquake Engineering 2: 1024–1041, ASCE.